Journal of Hydroscience and Hydraulic Engineering
Vol. 25, No.1 May, 2007, 21-30

NUMERICAL STUDY ON FINGERING FLOW IN NON-UNIFORM POROUS MEDIA

BY

Masahiko Saito

Research Center for Urban Safety and Security, Kobe University, Rokkodai-cho Nada, Kobe, Japan

SYNOPSIS

Fingering flow is known to occur in unsaturated sandy soil, yet numerical simulations are unable to reproduce this effect if the soil is assumed to be uniform. In this study, conventional saturated-unsaturated seepage analysis is performed using a coupled $1/f^{-\zeta}$ model as a geostatistical model of hydraulic conductivity. The results of this study provide strong evidence that when the mean hydraulic conductivity is relatively high, fingering flow can be simulated even though the variance of hydraulic conductivity is very low , This can be explained by the difference of water retention curves. The shapes of the flow paths can be characterized by fractal dimensions. When the mean hydraulic conductivity is relatively low, fingering flow rarely occurs, except in the case where the variance of the hydraulic conductivity is very high.

INTRODUCTION

Problems such as the vertical infiltration of rainfall into soil are generally handled by saturated-unsaturated seepage analysis using finite difference or finite element methods (Neuman (1), (2), Akai et al. (3)). However, the physical characteristics of soil exhibit wide scatter in the spatial distribution on both microscopic and macroscopic scales, and it is hard to measure the distributions of these parameters. Researchers are forced to assume constant values in the soil strata based on uniformity yielded by survey data at a limited number of locations. This remains a major obstacle to improving the reliability of simulations related to subsurface flow.

It is well known that fingering occurs during vertical infiltration flow under certain conditions, even in soils with little scatter in physical properties. It is impossible to simulate this fingering phenomenon if the soil characteristics are assumed to be exactly uniform.

Kawamoto *et al.*(4) identified relations among grain diameter, initial water content and flux, which correlate with the shapes of infiltration in laboratory experiments on fingering in soils that can be considered uniform. Furthermore, in laboratory experiments, Sakamoto(5),(6) verified that the shapes of fingering flow are fractal in nature, and proposed that the water path invasion model is capable of reproducing the infiltration pattern. This model employs networks of passages with varying diameters and lengths to imitate the structure of porous infiltration paths in unsaturated soils. The infiltration mechanisms are thus reproduced precisely on a microscopic scale. However, the parameters used in the Sakamoto's model differ from the unsaturated hydraulic conductivity and the water retention curve employed in general seepage analysis will be included in this study.

The present study combines the commonly used saturated-unsaturated seepage analysis with the special distribution model of soil physical parameters previously proposed by the authors(Saito and Kawatani(7), (8), (9)). A

simple and repeatable finite-element analysis of fingering phenomena during vertical seepage flow is attempted. Some observations are made on how the characteristics of the distribution of hydraulic conductivity and analytical scale are related to the shapes of infiltration.

GOVERNING EQUATION AND THE WATER RETENTION CURVE

Governing equation

The following Richards' equation (Richards (10)) is used as the governing equation:

$$\left(C+\beta S_s\right)\frac{\partial \psi}{\partial t}=\nabla\cdot\left[\mathbf{K}\cdot\left(\nabla\psi+\nabla Z\right)\right] \tag{1}$$

where C is the specific water capacity (= $\phi \mathrm{d}S_w/\mathrm{d}\psi$, where ϕ is porosity and S_w is saturation), S_s is specific storage coefficient, $\mathbf{K}$ is the hydraulic conductivity tensor, ψ is the pressure head, and Z is the elevation head. In the saturated zone ($S_w = 1$), $\beta = 1$, and in the unsaturated zone, ($S_w \neq 1$), $\beta = 0$. Also, $\mathbf{K}$ can be expressed as follows in terms of the relative permeability k_r and the saturated hydraulic conductivity **Ks**:

$$\mathbf{K} = k_r \cdot \mathbf{Ks} \tag{2}$$

The condition on boundary Γ_1, where the pressure is defined, is given by

$$\psi = \psi_1 \quad \text{on} \quad \Gamma_1 \tag{3}$$

On boundary Γ_2, where flux q is defined,

$$q = q_2 = -\mathbf{n}\cdot\mathbf{K}\cdot\left(\nabla\psi+\nabla Z\right) \quad on \quad \Gamma_2 \tag{4}$$

where $\mathbf{n}$ is the outwardly directed unit normal vector.

The Water Retention Curve

The relative permeability k_r is an essential parameter in the analysis of seepage. It is considered a function of saturation, and the saturation S_w is considered a function of capillary pressure ψ_c ($\equiv -\psi$). Of the many mathematical models proposed to describe these relationships (water retention curve), the van Genuchten equation (11) is employed in the present study:

$$S_e = \frac{S_w - S_r}{1 - S_r} = \left\{1+\left(\alpha\psi_c\right)^n\right\}^{-m} \tag{5}$$

where S_e is the effective saturation, S_r is the residual saturation, and α, n and m are parameters, where n and m are dimensionless and α has dimensions of the reciprocal of the pressure head. The parameters n and m are not independent, and they are related by

$$m = 1 - 1/n \tag{6}$$

The relative permeability and effective saturation are related as follows.

$$k_r = S_e^{\varepsilon}\left\{1-\left(1-S_e^{1/m}\right)^m\right\}^2 \tag{7}$$

where ε is a parameter related to the degree of interconnection among voids. Generally, a value of 0.5 is used for ε. Differentiation of Eq. (5) with respect to ψ_c and rearranging the result gives

$$C = -\phi \frac{dS_w}{d\psi_c} = \phi\alpha mn(1-S_r)(\alpha\psi_c)^{n-1}\left\{1+(\alpha\psi_c)^n\right\}^{-m-1} \tag{8}$$

Thus, the water retention curve and relative permeability can be calculated if the parameters α, n and the residual saturation S_r are determined.

MODEL OF SPATIAL DISTRIBUTION OF SOIL PROPERTIES

Spatial distribution of hydraulic conductivity

The authors have created a model of the spatial distribution of permeability based on a stochastic fractal model. The model takes the form $f^{-\zeta}$, as shown in the following equation for the spectral density of the logarithm of saturated hydraulic conductivity ($Y = \log(k_s)$). Researchers have shown that it is easy to model the spatial distribution of the hydraulic conductivity of actual soil using this model(Saito and Kawatani (7), (8), (9)).

$$S(|\boldsymbol{f}|) \propto |\boldsymbol{f}|^{-\zeta} \tag{9}$$

where $\boldsymbol{f}$ is the spatial frequency vector, $S(|\boldsymbol{f}|)$ is the power spectral density, and ζ is a parameter expressing the spatial correlation, where $\zeta \cong 2$ in a two-dimensional model. When the autocorrelation function is approximated with an exponential function, the integral scale becomes about 0.1 times the field length.

We know that the variance of Y in this model is proportional to the logarithm of the spatial resolution (number of elements in the model). That is, if M is the resolution and λ is a proportional constant, the variance can be expressed as follows:

$$\sigma^2 = \lambda \log_{10} M \tag{10}$$

where σ is the standard deviation of the natural logarithm of the hydraulic conductivity and M is the number of square elements making up the volume of interest.

Thus, the spatial distribution characteristics of this model are determined by the parameter ζ, which expresses the correlation, and λ, which expresses the magnitude of scattering.

Spatial Distribution of VG parameters

If van Genuchten's equation is used to describe the water retention curve, the parameters α, n and S_r must be determined. In this work we employ the laboratory results for sandy soil reported by Yanaka and Ishida(12) and the results for glass beads reported by Nakagawa *et al*(13). These results have been used previously (Saito and Kawatani (14)) to estimate the relationship between the saturated hydraulic conductivity k_s and α according to

$$\alpha^{-1} = -37.35 \times \log_{10} k_s - 16.22 \tag{11}$$

where the units are 1/cm for α and cm/s for k_s, and it is assumed that $\alpha^{-1} \geq 1.0$ cm. The general tendency is that as k_s increase, S_r becomes lower. S_r is thus assumed to be a function of k_s based on some measured examples[12]:

$$S_r = -0.15 \times \log_{10} k_s - 0.2 \tag{12}$$

where, $S_r \geq 0$ and is dimensionless, and k_s is in units of cm/s. As no clear correlation has been found between n and k_s, it was assumed that n is spatially constant.

Simulation Model

Figure 1 shows a diagram of the flow domain. The domain is two-dimensional, a square measuring $L \times L$ (dimensions in meters). The boundary conditions were as follows: Impervious boundaries at $x = 0$ and $x = L$, $q = 0$ at the seepage surface boundary ($z = 0$) when $\psi < 0$, and $\psi = 0$ when $q < 0$.

At the soil surface, flux q is set to 30.0 mm/h or ψ is set to 0 (= ambient atmospheric pressure) when the soil is saturated. Porosity ϕ is set to 0.25, the number of elements in the analytical mesh is 128 × 128, and the element size is L/128 m × L/128 m.

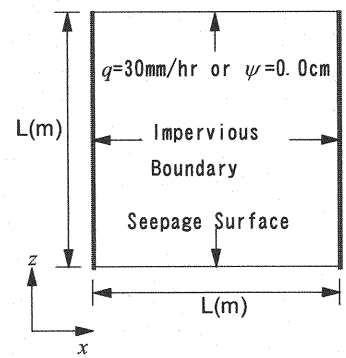

Fig. 1 Analytical domain

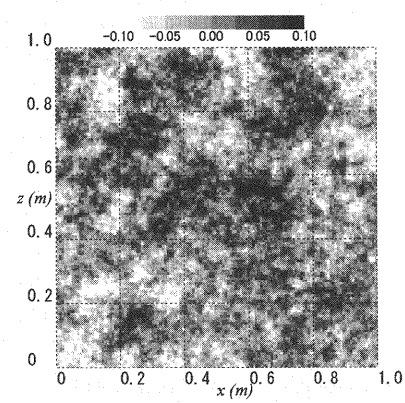

Fig. 2 Distribution of log (k_s/k_m)

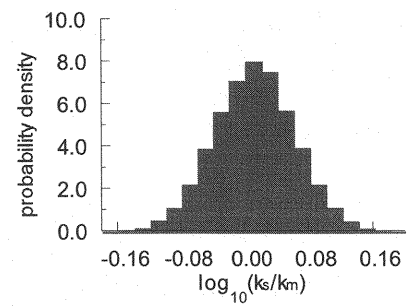

Fig. 3 Frequency (probability density) of log (k_s/k_m)

To determine the distribution of hydraulic conductivity, ζ is set to 2.0 in Eq. (9). Figures 2 and 3 show examples of the distributions of saturated hydraulic conductivity and frequency.

The events under analysis are classified into Case 1 and Case 2 according to the value of k_m, and are further subdivided as shown in Table 1 into a total of 6 cases depending on the other conditions.

Table 1 Conditions of analysis

	k_m(cm/s)	L(m)	σ	n	Initial Condition
Case-1a	0.3	1.0	0.05	7	ψ=-0.4 (m)
Case-1b		5.0			
Case-1c		1.0	0.10		
Case-2a	0.06	1.0	0.05	4	ψ=-1.5 (m)
Case-2b			0.40		
Case-2c		5.0			

RESULTS AND DISCUSSION

Case 1a ~1c

Several conditions which increase the likelihood of fingering have been established. For example, in coarse soil and when the initial water content is low (Miyazaki (15)). As permeability generally increases with grain diameter, 20% particle diameter (d_{20}) is assumed to be about 1.0mm and k_m is set to 0.3 cm/s by Creager method in Case 1a ~ 1c. According to the experiments by means of glass beads which have a similar permeability (Nakagawa et al. (13)), n is set equal to the measured value of 7. ψ is set to an initial value of –0.4m in order to obtain a saturation of approximately 0% throughout the area.

Figures 4 and 5 show the saturation distribution and velocity vector distribution 97 min after the initial time in these simulations. The magnitude of the velocity is shown normalized by k_m. These figures clearly indicate fingering flow. In Case 1a, σ is set to 0.05 ($\lambda = 5.93 \times 10^{-4}$), and the scatter in saturated hydraulic conductivity is quite small. These figures clearly show that the water ran preferentially through locations with lower permeability (white areas in Fig. 2).

The value of α^{-1} calculated using Eq. (11) is 3.31 1/cm at $k_m = 0.3$ cm/s. If k_m is increased by σ, i.e., $k_{+\sigma} = 0.337$ cm/s, α^{-1} becomes 1.42 cm, and if decreased by σ, $k_{-\sigma} = 0.267$ cm/s, $\alpha^{-1} = 5.20$ cm. Thus, the magnitude of α^{-1} varies by a factor of 3.70 within a range of $\pm\sigma$. This indicates significant scatter in the water retention curve, as shown in Figure 6. Figure 7 shows a plot of ψ_c with respect to soil water diffusivity ($D = k_r \times k_s/C$). This plot reveals severe scatter in the soil water diffusivity in soils with identical capillary pressures. If the relationship in Eq. (11) is assumed, it is clear that D grows with decreasing hydraulic conductivity. Therefore, even if there is low scatter in the hydraulic conductivity, large discrepancies appear in the water retention curve at low ranges of α^{-1}. As particularly large discrepancies occur for soils with identical capillary pressures, it appears likely that the flows are concentrated in partial area.

Figure 8 shows the saturation distribution in Case 1b (domain expanded by a factor of 5), and Figure 9 shows the saturation distribution in Case 1c, where $\sigma = 0.1$ ($\lambda = 2.37 \times 10^{-3}$). The data for both figures are those for the condition immediately prior to the moment when the flow reached the bottom of the domain. Expansion of the analytical domain (Case 1b) involves an expansion of the mesh size. Small-scale fingering flow is, therefore, not accurately reproduced. However, it is clear that large fingering flows did occur in this case. This result is expected if the shape of fingering flow is assumed to be fractal in nature. As the hydraulic conductivity was given high scatter in Case 1c, the central area of the analytical domain, in which conductivity was high, exhibits lower soil water diffusivity and the finger penetration was shorter than in Case 1a.

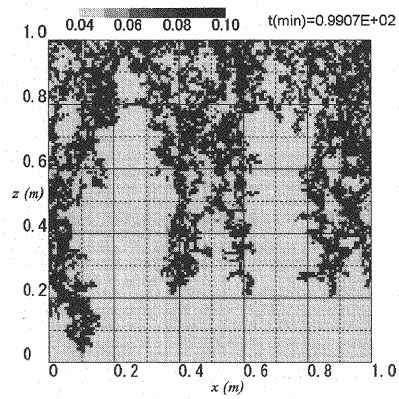

Fig. 4 Saturation distribution (Case-1a)

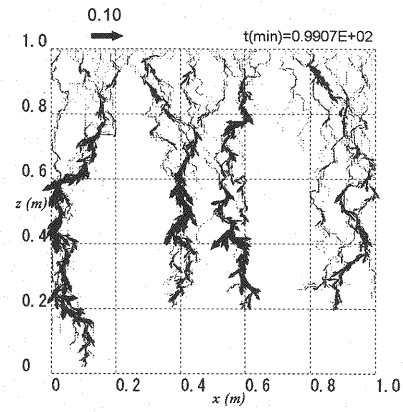

Fig. 5 Velocity vector distribution (Case-1a)

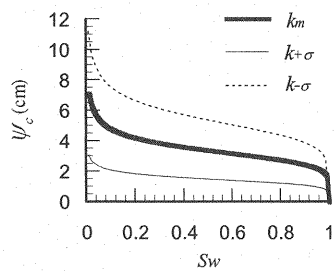

Fig. 6 Water retention curves

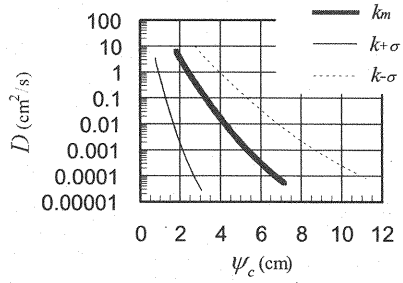

Fig. 7 Soil water diffusivity

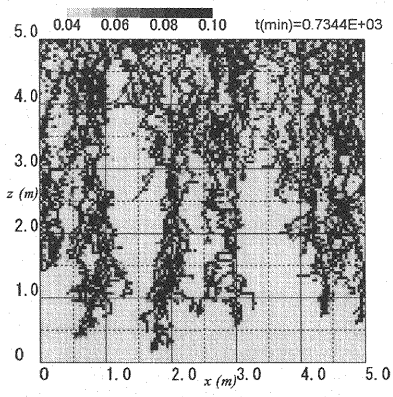

Fig. 8 Saturation distribution (Case-1b)

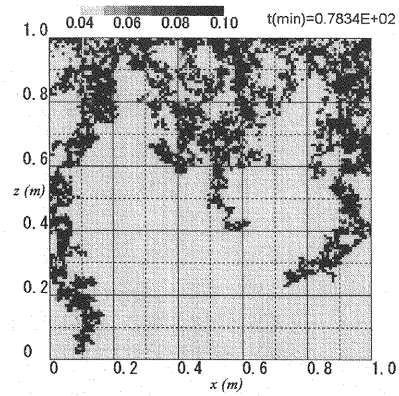

Fig. 9 Saturation distribution (Case-1c)

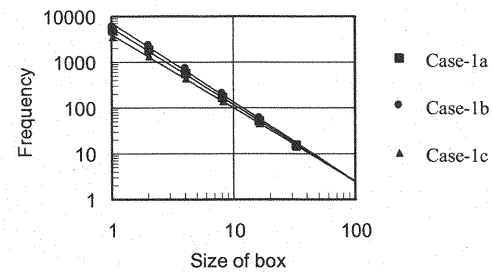

Fig. 10 Estimation of fractal dimension by the box counting method

The fractal dimensions of the saturation distributions seen in the fingers shown in Cases 1a to 1c (immediately prior to reaching the bottom) were estimated by a box counting method (Figure 10). The threshold condition for saturation in this calculation was $S_w > 0.05$. The fractal dimensions were calculated from the linear regression lines provided in Figure 10. The obtained dimensions were 1.68 for Case 1a, 1.73 for Case 1b, and 1.60 for Case 1c. These results are in general agreement with those found by Sakamoto(6) in simulations of wide-area flow.

Case 2a ~2c

The saturated hydraulic conductivity in Case 2 is set to 1/5 the value employed in Case 1, and n is set to 4 to simulate an increase in the fine soil fraction. The initial value of ψ is set to –1.5 m in all cases to ensure that saturation of the overall analytical area would reach a value close to the residual saturation. Figure 11 shows the flow velocity vector distribution for Case 2a. No distinguishable fingering occurred in this case, in contrast, to that shown in Figure 5. This reflects the characteristics of wide-area flow, and is achieved by setting the mean saturated hydraulic conductivity k_m to 1/5 the value employed in Case 1. In this case, the scatter in the water retention curve exhibits slight scatter in comparison to the results for $\sigma = 0.05$. As seen in Case 1, lower k_m results in a broader flow speed distribution.

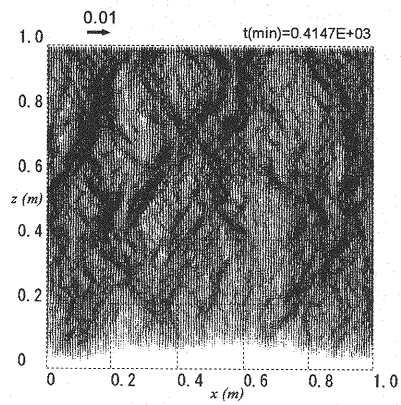

Fig. 11 Velocity vector distribution (Case-2a)

In Case 2b, σ was set to 0.4 ($\lambda = 3.80 \times 10^{-2}$) such that the scatter in α within $k_s = k_m \pm \sigma$ would be similar to that seen in Case 1a. Figure 12 shows the flow velocity vector distribution in Case 2b. The flow was concentrated in a partial area (dominant localized flow), as seen in Case 1a. Nevertheless, the flow was much more meandering than in Case 1a, with some branches proceeding in a horizontal direction. Figure 13 shows the saturation distribution. No distinguishable fingering flow occurred in this case, in contrast to Case 1, due to scatter in the residual saturation S_r described by Eq. (11) and the extreme scatter in the initial saturation resulting from the initial pressure head of $\psi = -1.5$ m. The high scatter in the initial saturation caused a persistent effect throughout the experiments.

Figure 14 shows the flow velocity vector distribution in the 5 m × 5 m numerical domain for Case 2c. This pattern differs markedly from that in Fig. 12 for Case 2b in that there is no clear self-similarity, as was seen in Case 1. These results demonstrate that the size of the analytical domain affects the shape of seepage flow.

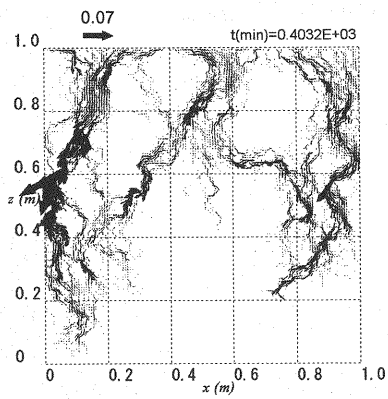

Fig. 12 Velocity vector distribution (Case-2b)

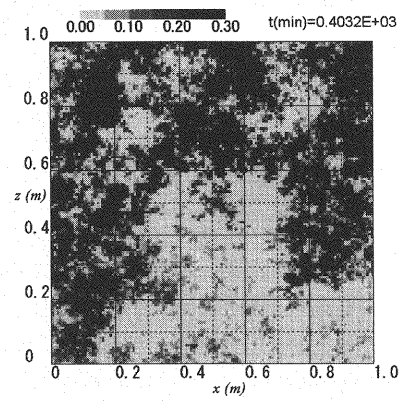

Fig. 13 Saturation distribution (Case-2b)

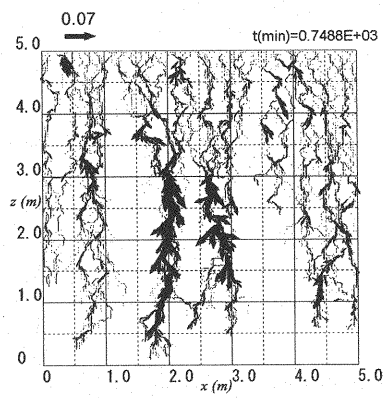

Fig. 14 Velocity vector distribution (Case-2c)

CONCLUSIONS

In this study, saturated-unsaturated seepage analysis was combined with the spatial distribution model of soil properties in an attempt to reproduce the fingering flow characteristics of vertical seepage flows and to observe relationships between the shapes of vertical seepage and conditions such as the distribution of saturated hydraulic conductivity and domain size. The main conclusions of this study are as follows.

1) Given a hydraulic conductivity distribution with high mean value, even a subtle variance can cause large differences in the water retention curve and extreme scatter in the soil water diffusivity, resulting in the concentration of flow in partial area. The parameter α, which describes the shape of the water retention curve, also exhibits a relatively strong correlation with the saturated hydraulic conductivity. Fingering occurs in domains with high values of α^{-1} (i.e., domains with low permeability).
2) Findings show that description of the shape of fingering flow in terms of the saturation distribution produces a fractal shape. It is therefore possible to predict that larger analytical scales result in larger fingering channels.
3) Hydraulic conductivity distributions with low mean values are less likely to result in fingering flow. However, when there is large scatter in the water retention curve (i.e., when there is wide variance in the distribution of hydraulic conductivity), the flow shape is dominantly local flow. However, the saturation distribution does not display any distinct fingering, and the scale of the analytical domain affects the predicted flow shape.

REFERENCES

1. Neuman, S. P.: Saturated unsaturated seepage by finite elements, *Proc., ASCE HY*, Vol.99, No.12, pp.2233-2250, 1973.
2. Neuman, S. P.: Galerkin method of analyzing non-steady flow in saturated-unsaturated porous media, *Finite element Method in flow problem*, edited by C. Taylor, O.C. Zienkiewicz, R.H. Gallagher, John Wiley & Sons, Chap.19, 1974.
3. Akai, K., Ohnishi, Y. and Nishigaki, M.: Finite Element Analysis of Saturated-Unsaturated Seepage in Soil, *Proceedings of the Japan Society of Civil Engineering*, No.264, pp.87-96, 1977.
4. Kawamoto, K., Miyazaki, T. and Nakano, M.: Leaching Efficiency Depending on the Type of Fingering Flow in Sandy Soils, *Trans. of JSIDRE*, No.186, pp.89-96, 1996.
5. Sakamoto, Y.: Fractal Dimension of Water Path through Unsaturated Media and Its Simulation using Water Path Invasion Model, *Proceedings of Hydraulic Engineering*, vol.36, pp.447-452, 1992.
6. Sakamoto, Y.: Simulation of Water Path through Unsaturated Media by Water Path Invasion Model involving Effects of Angle of Contact and Water Content, *Proceedings of Hydraulic Engineering*, Vol.38, pp.179-184, 1994.
7. Saito, M. and Kawatani, T.: Theoretical Study on Spatial Distribution of Hydraulic Conductivity, *Journal of Geotechnical Engineering*, No.645/Ⅲ-50, pp.103-114, 2000.
8. Saito, M. and Kawatani, T.: Study on Applicability of Geostatistical Models of Hydraulic Conductivity, *Journal of Geotechnical Engineering*, No.694/Ⅲ-57, pp.245-258, 2001.
9. Saito, M. and Kawatani, T. : Study on statistical properties of 1-D random permeability fields generated by stochastic fractal model, *Journal of Applied Mechanics*, JSCE, Vol.5, pp.491-498, 2002.
10. Richards, L. A.: Capillary Conduction of Liquids through Porous Mediums, *Physics*, 1, pp.318-333, 1931.
11. van Genuchten, M. T.: A closed-form equation for predicting the hydraulic conductivity of unsaturated soils, *Soil Science Society of America Journal*, Vol.44, pp.892-898, 1980.
12. Yanaka, H. and Ishida, T.: An examination of relative permeability curve (θ-k, relationship) of sandy soil, *Proceedings of the Thirty-Third Japan National Conference on Geotechnical Engineering*, Vol.2, pp.1817-1818, 1998.
13. Nakagawa, K., Iwata, M., Chikushi, J. and Momii, K.: Unsaturated water flow and solute transport in artificially distributed hydraulic conductivity field, *Journal of Hydroscience and Hydraulic Engineering*, Vol.21, No.2, pp.37-45, 2003.
14. Saito, M. and Kawatani, T.: Two-Phase Flow Simulation of Rainfall Infiltration and Seepage Processes Considering Heterogeneity of Hydraulic Conductivity, *Journal of Hydroscience and Hydraulic Engineering*, Vol.23, No.1, pp.67-76, 2005.
15. Miyazaki, T.: Environmental Soil Hydrology, *University of Tokyo Press*, pp.36-37, 2000.

APPENDIX – NOTATION

The following symbols are used in this paper:

C = specific water capacity;

D = soil water diffusivity;

$\boldsymbol{f}$ = spatial frequency vector;

k_m = mean value of saturated hydraulic conductivity;

k_r = relative permeability;

k_s = saturated hydraulic conductivity;

$\mathbf{K}$ = hydraulic conductivity tensor;

$\mathbf{K}_s$ = saturated hydraulic conductivity tensor;

m = VG parameter;

M = resolution;

n = VG parameter;

$\mathbf{n}$ = outwardly directed unit normal vector;

q = flux;

S_e = effective saturation;

S_r = residual saturation;

S_s = specific storage coefficient;

S_w = degree of saturation;

t = time;

x, z = Cartesian coordinates;

Z = elevation head;

α = VG parameter;

ε = parameter related to the degree of interconnection among voids;

ζ = parameter expressing the spatial correlation;

λ = proportional constant;

σ = standard deviation of the logarithm of the hydraulic conductivity

ϕ = porosity;

ψ = pressure head;

ψ_c = capillary pressure;

(Received July 28, 2006 ; revised December 6, 2006)